Article

The Effects of Dissolved Halide Anions on Hydrogen Bonding in Liquid Water

Jared D. Smith, Richard J. Saykally, and Phillip L. Geissler

J. Am. Chem. Soc., **2007**, 129 (45), 13847-13856• DOI: 10.1021/ja071933z • Publication Date (Web): 25 October 2007

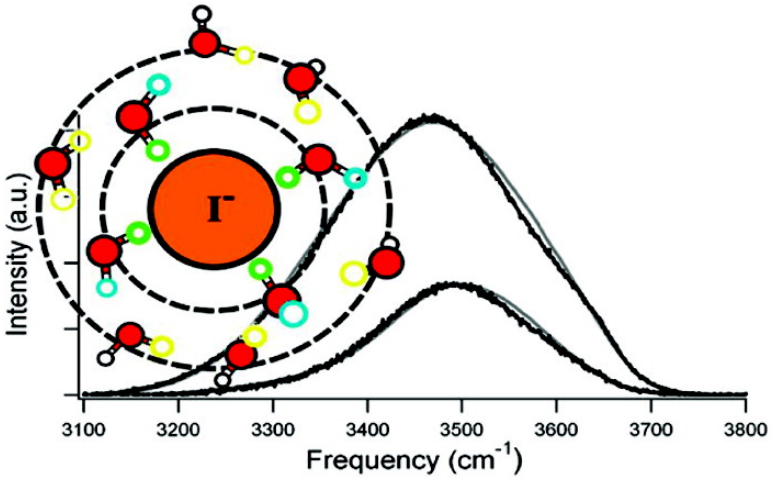

More About This Article

Additional resources and features associated with this article are available within the HTML version:

- Supporting Information
- Links to the 13 articles that cite this article, as of the time of this article download
- Access to high resolution figures
- Links to articles and content related to this article
- Copyright permission to reproduce figures and/or text from this article

View the Full Text HTML

J|A|C|S
ARTICLES
Published on Web 10/25/2007

The Effects of Dissolved Halide Anions on Hydrogen Bonding in Liquid Water

Jared D. Smith,[†,‡] Richard J. Saykally,[†,‡] and Phillip L. Geissler*[,†,‡,§]

Contribution from the Department of Chemistry, University of California, Berkeley, California 94720, and Chemical and Material Sciences Divisions, Lawrence Berkeley National Laboratory, Berkeley, California 94720

Received March 19, 2007; E-mail: geissler@berkeley.edu

Abstract: It is widely believed that the addition of salts to water engenders structural changes in the hydrogen-bond network well beyond the adjacent shell of solvating molecules. Classification of many ions as "structure makers" and "structure breakers" has been based in part on corresponding changes in the vibrational spectra (Raman and IR). Here we show that changes in O−H vibrational spectra induced by the alkali halides in liquid water result instead from the actions of ions' electric fields on adjacent water molecules. Computer simulations that accurately reproduce our experimental measurements suggest that the statistics of hydrogen-bond strengths are only weakly modified beyond this first solvation shell.

Introduction

The physical and chemical properties of ions in aqueous solution are centrally important for many biological, geological, environmental, and industrial processes.[1] Yet despite enormous efforts, several important issues remain unresolved regarding the microscopic structure of the surrounding solvent and associated chemical consequences for even the simplest of ions. In particular, a distinction has often been suggested between ions that induce stronger hydrogen bonds (HBs) in their surroundings ("structure makers") and ions that weaken or distort nearby HBs ("structure breakers"). Although this widely held notion has been used to rationalize many diverse observations, its basis is entirely empirical, and in most cases, it remains unclear why a particular ion acts as a "structure maker" or as a "structure breaker".

Available experimental techniques cannot directly resolve the arrangements of HBs in the vicinity of a solvated ion. For this reason, intermolecular structure has been inferred from various thermodynamic and spectroscopic data. For example, changes in water's neutron diffraction pattern, upon addition of ions, resemble those effected by applying high pressure.[2] In the case of elevated pressure, those changes reflect strong distortion of HBs throughout the liquid. It has therefore been suggested that ions strongly influence HB strength and geometry even for molecules beyond the first solvation shell. Similar conclusions have also proceeded from Raman studies of aqueous solutions[3] and from the "apparent density" of salt solutions.[4] (The "apparent density" is defined as the calculated density of the liquid after the mass and volume associated with the ions have been removed from the solution.[4]) In contrast, recent ultrafast infrared pump−probe measurements appear to indicate that dissolved ions only significantly affect vibrational and orientational relaxation times of water molecules in the first hydration shell,[5,6] implying that structural rearrangements are strongly localized. Resolving such ambiguities requires quantitative connections between experimental observables and the statistics of HB geometries.

In this contribution we address the intermolecular rearrangements that accompany solvation of anions (specifically halides) in aqueous solution, using Raman spectroscopy of water's O−H stretch vibrations together with computer simulations. Probes of water O−H stretching vibrations are useful for examining salt solutions because their spectra are extremely sensitive to the identities of dissolved anions.[3,7−11] In fact, the shape and location of vibrational line shapes often form the basis for classifying ions as "structure makers" or "structure breakers".[8,11] Implicit in this categorization is an assumed connection between O−H stretching frequency and the solvent's HB structure.

Here we challenge this widely held assumption. Specifically, we show that the difference between spectral line shapes of pure liquid water and those of most potassium halide solutions arise primarily from electric fields, along the OH bond, experienced by hydrogen atoms that are proximal to an anion. Because water molecules in the ion's first solvation shell are strongly oriented, these hydrogen atoms cannot participate in HBs with other water molecules. In this sense anions undoubtedly have a distinct, but

† Department of Chemistry, University of California, Berkeley.
‡ Chemical Sciences Division, Lawrence Berkeley National Laboratory.
§ Material Sciences Division, Lawrence Berkeley National Laboratory.

(1) Franks, F., Ed. *The Physics and Physical Chemistry of Water*; Plenum Press: New York, 1972; Vol. 1.
(2) Leberman, R.; Soper, A. K. *Nature* **1995**, *378*, 364.
(3) Dillon, S. R.; Dougherty, R. C. *J. Phys. Chem. A* **2002**, *106*, 7647.
(4) Dougherty, R. C. *J. Phys. Chem. B* **2001**, *105*, 4514.
(5) Omta, A. W.; Kropman, M. F.; Woutersen, S.; Bakker, H. J. *Science* **2003**, *301*, 347.
(6) Kropman, M. F.; Bakker, H. J. *Science* **2001**, *291*, 2118.
(7) Fischer, W. B.; Fedorowicz, A.; Koll, A. *Phys. Chem. Chem. Phys.* **2001**, *3*, 4228.
(8) Walrafen, G. E. *J. Chem. Phys.* **2005**, *123*.
(9) Terpstra, P.; Combes, D.; Zwick, A. *J. Chem. Phys.* **1990**, *92*, 65.
(10) Schultz, J. W.; Hornig, D. F. *J. Phys. Chem.* **1961**, *65*, 2131.
(11) Nickolov, Z. S.; Miller, J. D. *J. Colloid. Interface Sci.* **2005**, *287*, 572.

extremely local, effect on HB structure. The issue we address here is whether hydroxyl groups that are not directly associated with the ion, and that are therefore free to form HBs, tend to engage with other water molecules more or less extensively than in the pure solvent. Our results indicate that this influence of ion solvation on HB geometries, as reflected in Raman spectra, is quite weak.

Our analysis of measured Raman spectra and of computer simulations is focused on the internal electric fields present in salt solutions. More specifically, we consider the electrostatic force acting on each hydrogen atom due to surrounding molecules and ions, in the direction of the covalent O−H bond. It has been shown that this electric field component E is very nearly proportional to O−H frequency shift (from the gas-phase value) in an empirical molecular model of HOD in liquid D_2O.[12−14] (The scarcity of H atoms in such a dilute isotopic mixture ensures that O−H stretching is a well-defined vibrational mode, widely separated in frequency from O−D stretching in the same and neighboring molecules.) To the extent that the vibrational line shape is dominated by inhomogeneous broadening, and that the transition polarizability is invariant with configuration,[14] this proportionality allows the O−H stretch Raman spectrum to be interpreted simply and unambiguously: The normalized scattering intensity at frequency ω reports the probability that a given hydrogen atom experiences a corresponding electric field along the O−H bond. We have recently exploited this relationship in studying the temperature-dependent Raman spectrum of HOD in H_2O (and in D_2O).[15] In that work, we showed that the thermal distribution $P(E)$ of electric field strength, calculated from Monte Carlo simulations of SPC/E water, exhibits the experimentally observed isosbestic (temperature invariant) point, and the extracted van't Hoff energy. Each of these observations has been previously, and erroneously, interpreted to be a signature of two-state (or multistate) behavior.

Vibrational spectra of aqueous electrolyte solutions cannot be understood in quite such simple terms. Water molecules adjacent to an ion might differ from distant molecules not only in their electric field statistics but also in their Raman scattering cross sections. Nonetheless, the principal approximations used in ref 12 to arrive at the proportionality between E and ω, which are based on the distinction between intra- and intermolecular energy scales, remain equally valid for salt solutions. With these controlled approximations, Monte Carlo simulations of fluctuating solvation structure, and calculations of Raman intensity employing density functional theory, we have determined Raman spectra for model aqueous halide solutions at ambient conditions. The nearly quantitative agreement we have found with experiment suggests that the empirical molecular models employed correctly describe the essential microscopic features of anion solvation.

HB patterns in our model systems do not support a meaningful designation of "structure maker" or "structure breaker" for any of the halides we have investigated (F^-, Cl^-, Br^-, and I^-). Instead, each ion induces an arrangement of water molecules in the first solvation shell that is atypical for the pure liquid. The surrounding solvent adapts remarkably well to these uncommon structures, such that the number and strength of HBs in regions near each ion are distributed much as in the pure liquid. Electric field distributions near the ions do, however, deviate strongly from that of pure liquid water, primarily due to the bare ionic field. These deviations are further enhanced in Raman spectra of halide solutions by augmented transition polarizabilities, which can be larger than values typical of bulk water by up to a factor of 3. A comprehensive and accurate picture of Raman scattering from aqueous halide solutions is thus obtained without invoking any significant long-range distortion or reinforcement of the aqueous HB network, but rather, a careful accounting of the electrostatic forces that govern fluctuations in O−H stretching frequency.

Methods

The experimental methods employed here are similar to those previously described for measurements of pure water.[15] Briefly, we have recorded the room-temperature Raman spectra, in the −OH stretching region, of 14% (by mole) HOD in D_2O containing 1 M KX (X = F, Cl, Br, and I) (Aldrich 99+%). The 514.5-nm line of an Ar^+ ion laser (Coherent Inova 300), with an output power of 500 mW, was used as the light source. All polarizations of the scattered light were collected at 90° to the incoming beam and were dispersed with a 500-mm triple grating monochromator (Acton Spectapro 2500i). Detection was accomplished with a liquid nitrogen-cooled CCD detector (Princeton Instruments Spec10). The spectral resolution was approximately 15 cm^{-1}.

We have used standard Monte Carlo techniques to sample configurations of salt solutions from a classical, isothermal−isobaric ensemble. Our system comprises one halide ion and 107 rigid water molecules, all periodically replicated in space. Interactions between water molecules were computed from the SPC/E model,[16] whose charges and Lennard-Jones parameters were also used to determine ion−water interactions according to models developed by Dang.[17] While different models of intermolecular forces in liquid water have yielded different spectroscopic predictions, the electric field distributions on which we focus have shapes that are quite similar among a wide range of models. (See, for example, results in refs 18, 19.) Shifts in these distributions due directly to Coulombic interactions with a halide ion, determined primarily by the ion's size and charge, are also likely to be insensitive to precise model details. We thus expect that our specific choice of model, made for the sake of simplicity, does not strongly influence the nature of our results and conclusions.

We have also not represented counterions explicitly: Their contribution to the electric field on H atoms is expected to be small, since covalent OH bonds are almost invariably oriented away from cations,[20] with the hydrogen atoms correspondingly located at longer distances from the charges. This expectation is consistent with the observation that measured Raman spectra are independent of counterion identity for different monovalent cations (e.g., Li, Na, K, Cs).[9,10] Cations' presence is, however, implicit in discarding the zero wave vector term of Ewald sums, which would diverge if the periodically replicated system were to bear net charge. Imposing charge neutrality at zero wave vector is mathematically equivalent to introducing a spatially uniform distribution of positive charge.

For each ion, 10^6 Monte Carlo sweeps were performed at a temperature of 298 K and 1 atm pressure. We generated trial

(12) Eaves, J. D.; Tokmakoff, A.; Geissler, P. L. *J. Phys. Chem. A* **2005**, *109*, 9424.
(13) Fecko, C. J.; Eaves, J. D.; Loparo, J. J.; Tokmakoff, A.; Geissler, P. L. *Science* **2003**, *301*, 1698.
(14) Corcelli, S. A.; Skinner, J. L. *J. Phys. Chem. A* **2005**, *109*, 6154.
(15) Smith, J. D.; Cappa, C. D.; Wilson, K. R.; Cohen, R. C.; Geissler, P. L.; Saykally, R. J. *Proc. Natl. Acad. Sci. U.S.A.* **2005**, *102*, 14171.
(16) Berendsen, H. J. C.; Grigera, J. R.; Straatsma, T. P. *J. Phys. Chem.* **1987**, *91*, 6269.
(17) Dang, L. X. *J. Phys. Chem. B* **2002**, *106*, 10388.
(18) Harder, E.; Eaves, J. D.; Tokmakoff, A.; Berne, B. J. *Proc. Natl. Acad. Sci. U.S.A.* **2005**, *102*, 11611.
(19) Schmidt, J. R.; Corcelli, S. A.; Skinner, J. L. *J. Chem. Phys.* **2005**, *123*.
(20) Neilson, G. W.; Mason, P. E.; Ramos, S.; Sullivan, D. *Philos. Trans. R. Soc. London, Ser. A* **2001**, *359*, 1575.

displacements of each molecule's position and orientation by adding a random vector to its center of mass and rotating it about a Cartesian axis by a random amount. These random displacements were drawn from Gaussian distributions, with standard deviations of 0.09 Å for translations and 12.6° for rotations, yielding average acceptance probabilities of roughly 40%. Ions were moved in the same way but, possessing spherical symmetry, were not rotated.

In the classical equilibrium distributions we sample, there is no distinction between H and D isotopes: We are free to replace any proton with a deuteron. To compute vibrational spectra of HOD in D_2O, we effectively made this replacement at all but one site and computed its vibrational frequency. Since the tagged H site is chosen arbitrarily, the procedure can be repeated with different choices. Each configuration thus provides 2×107 different OH bonds that play the role of the probed stretching vibration, so that statistical averages converge quickly.

Within first-order perturbation theory and a linearization of the coupling between the chosen oscillator and its bath (i.e., all other molecules and the ion), the OH vibrational frequency (ω) is shifted from its gas-phase value (ω_0) by an amount

$$\Delta\omega = \omega - \omega_0 = QE \tag{1}$$

Here E is the electric field evaluated at the H atom of interest and projected onto the OH bond. This electric field component can be written in terms of distances between the tagged H atom and all other charged sites in the system, including the ion,

$$E = \hat{\mu} \cdot \sum_{i=1}^{n} \frac{q_i \hat{r}_{i\mathrm{H}}}{r_{i\mathrm{H}}^{\,2}} \tag{2}$$

Here the sum is over all charge sites in the simulation, $\hat{\mu}$ is a unit vector along the tagged OH bond, $\hat{r}_{i\mathrm{H}}$ is a unit vector pointing from site i to the H atom, q_i is the charge on site i, and $r_{i\mathrm{H}}$ is the distance from site i to the H atom.

The slope (Q) and intercept (ω_0) of $\omega(E)$ in eq 1 have previously been computed as (a) the difference between ground- and excited-state dipoles of an isolated HOD molecule, and the gas-phase vibrational frequency, respectively,[12] or (b) empirical parameters determined from electronic structure calculations on small water clusters.[14] In this paper, we treat Q and ω_0 as empirical parameters fixed by the Raman spectrum of pure HOD in D_2O.

By computing E for different H atoms in many different configurations, we determined frequency distributions for specific regions near the anion. We make this spatial separation because Raman intensities vary, depending on the proximity to the ion, and because the relative numbers of oscillators in each region depend on ion concentration, which is not conveniently controlled in these simulations. We ultimately constructed Raman spectra to compare with experiment by adding these spatially resolved distributions, weighted both by their Raman intensities and by their relative populations at a given ion concentration.

Perhaps the most serious approximation we have made in this computational procedure is the neglect of dynamical effects on the OH Raman spectrum, specifically, motional narrowing. Librational motions, in particular, occur on time scales shorter than the inverse width of the equilibrium frequency distribution.[1] In classical molecular dynamics simulations, rapid bath fluctuations indeed reduce the spectral line width by approximately 30%.[12] The spectroscopic calculations presented here instead assume a static environment for each oscillator. We adopt this approach for two reasons. First, the static distribution we have computed admits a straightforward physical interpretation that might be obscured by motional narrowing. Second, fluctuations at frequencies sufficiently high to affect the line shape noticeably are likely to be strongly quantized, modifying their dynamic contributions in ways that are difficult to calculate or anticipate. Electric field distributions we and others have reported, in fact, resemble measured spectra more closely than when classical bath dynamics is explicitly considered (see refs 12 and 15 for examples). The standard strategy for including dynamical effects on OH vibrations in water might therefore systematically overestimate their influence on spectral shape and/or width. In this sense, the parameter Q we use to map electric field distributions into predicted Raman line shapes could be viewed as an empirical but accurate account of rapid fluctuations in the aqueous environment. We in effect assume that bath dynamics, when properly taken into account, change the width but not the shape of vibrational spectra and further that this scaling of spectral line width does not depend on the presence or absence of a monovalent anion.

Although it has been shown that the Raman intensity of HOD in pure water is relatively insensitive to variation in its hydrogen-bonding environment,[14] direct interaction of HOD molecules with an anion (i.e., DOH···X) can have a dramatic effect on the Raman intensity. In fact, the measured Raman intensity for KX solutions (I_X) has been observed to increase across the halide series (i.e., $I_F < I_{Cl} < I_{Br} < I_I$).[10] This effect is thought to result primarily from water molecules directly bonded to the anion and is related to the OH···X bond polarity.[10] It is essential to account for this effect in order to compare our calculations directly to the measured Raman spectra. We therefore determined numerically the Raman intensities of OH oscillators directly bonded to an anion relative to an oscillator in pure water (i.e., $I_{OH\cdots X}/I_{OH\cdots OH2}$). These relative Raman intensities were calculated using the GAUSSIAN 03 software package[21] employing a method very similar to the one recently described by Corcelli et al. for Raman calculations on pure water.[14] In detail, we extracted configurations of small clusters, containing the anion and its first solvation shell (6−8 water molecules), from snapshots of the MC simulations described above. The hydrogen of interest was then replaced with a deuterium, and the energy of the cluster was minimized with respect to OD bond length. This is accomplished by optimizing the geometry of the cluster while the positions of all atoms, other than the D atom of interest, were held fixed. We then calculated the frequency and Raman intensity of the OD stretching mode. The Raman intensity is calculated in GAUSSIAN by numerical differentiation of the analytically computed dipole moment derivatives with respect to an applied electric field. This calculation was repeated for a number of OD bonds in each cluster. Calculations on clusters containing F^-, Cl^-, and Br^- were performed using DFT at the B3LYP/6-311++G** level of theory,[22,23] and the B3LYP/LANLDZdp[24] level of theory was employed for the I^- cluster. For comparison, the Raman intensity of the OD stretch in $HOD(H_2O)_8$ clusters, was calculated at both levels of theory. It should be pointed out that these calculations apply equally well to an OH stretch in a D_2O cluster because the Raman intensity is an electronic property that is independent of isotopic mass. Similar calculations performed on fully optimized HOD···X dimers yielded relative Raman intensities within 3% of the values obtain from the larger cluster calculations, indicating that the effect is a very localized one. Indeed, calculated Raman intensities for H atoms near, but not adjacent to, X ions in small clusters are similar to values typical of the pure liquid.

Results and Discussion

The effect on the HOD Raman spectrum from the addition of 1 M KX is demonstrated by Figure 1. For KI, a dramatic blue-shift in peak intensity is observed, as well as a decrease in peak width (fwhm), which results in a more symmetric band profile as compared with that of pure HOD/D_2O. This effect becomes less pronounced across the halide series from I^- to Cl^-. In contrast, the KF spectrum actually shows a slight increase in peak width, with a small increase in intensity on

(21) Frisch, M. J.; et al. *Gaussian 03*; Gaussian, Inc.: Wallingford, CT, 2004.
(22) Becke, A. D. *J. Chem. Phys.* **1993**, *98*, 1372.
(23) Lee, C. T.; Yang, W. T.; Parr, R. G. *Phys. Rev. B* **1988**, *37*, 785.
(24) Check, C. E.; Faust, T. O.; Bailey, J. M.; Wright, B. J.; Gilbert, T. M.; Sunderlin, L. S. *J. Phys. Chem. A* **2001**, *105*, 8111.

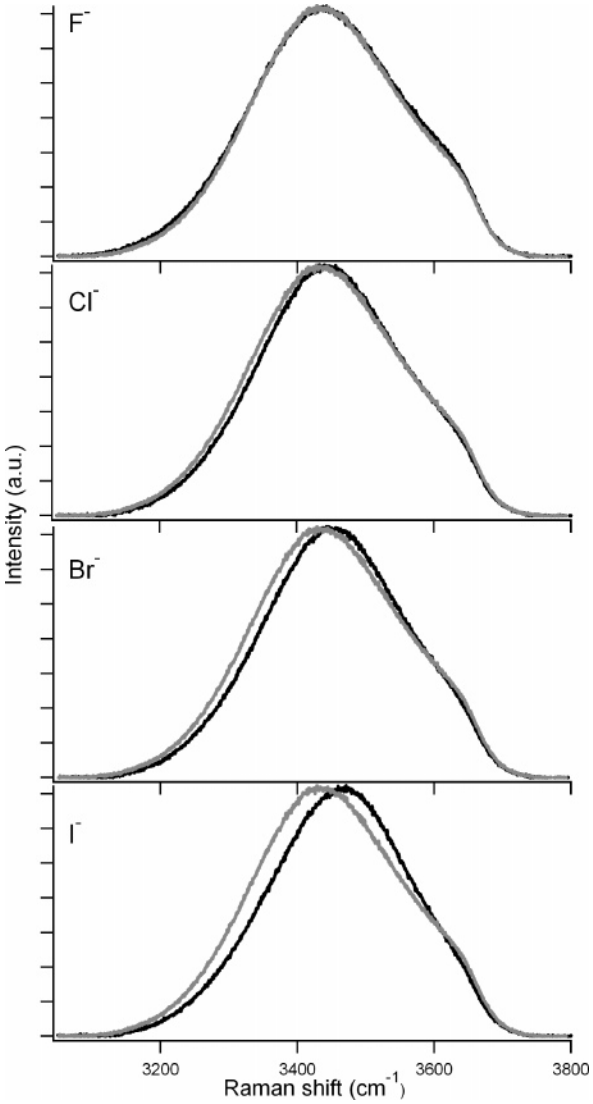

Figure 1. The −OH stretch Raman spectra for 1 M KX (X = F^-, Cl^-, Br^-, and I^-) in HOD/D_2O (black lines). Each spectrum is compared to the Raman spectrum of pure HOD/D_2O (gray lines). The peak intensities of each KX spectra are scaled to be the same as the pure HOD/D_2O spectra for better comparison.

the red side of the spectrum (<3300 cm^{-1}). This leads to a small red-shift of the spectrum at higher KF concentrations (not shown). In general, all of the changes observed in the 1 M salt solutions (compared to pure water) foreshadow the more dramatic changes observed at higher KX concentrations. Furthermore, these changes in the Raman spectrum are quite similar to those reported for the FTIR spectrum when KF or KI are added to HOD/H_2O[11]. In that particular study, the observed changes to the FTIR spectra were interpreted as "proof" that these salts have a significant "structure making" (KF) or "structure breaking" (KI) effect on the surrounding HB network.[11]

To clarify anions' effects on solvent structure, we classify H atoms in our computer simulations according to their distance r from the ion. Those with $r < r_1$ (corresponding to the first peak of the H−X radial distribution function, $g_{HX}(r)$, calculated from computer simulations) and those with $r_1 < r < r_2$ (corresponding to the second peak of $g_{HX}(r)$) experience the largest changes in structure and electric field relative to the pure liquid. Here r_1 and r_2 correspond to the first and second minima

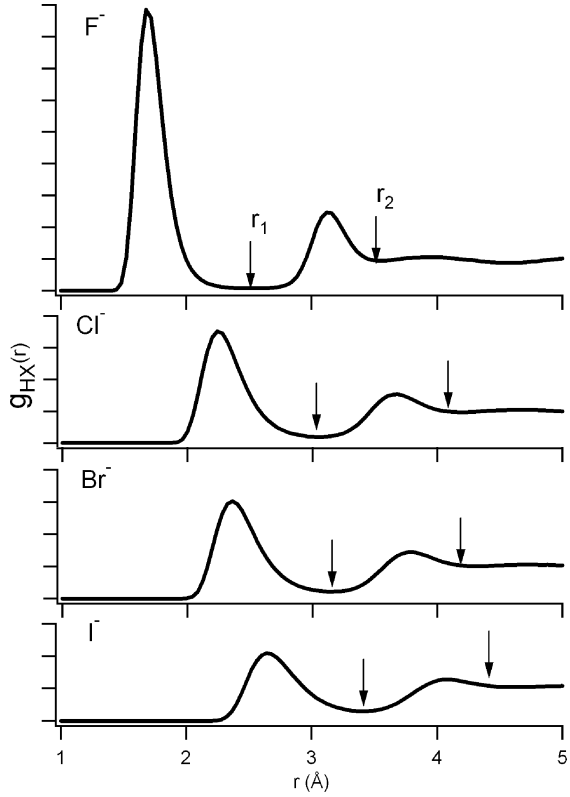

Figure 2. H−X pair distribution functions calculated for each anion. The radial cutoffs r_1 and r_2 we use to distinguish various populations are indicated with arrows. H atoms closer than r_1 are in the first hydration shell and are directed toward the anion to form near-linear OH···X hydrogen bonds. The H atoms between r_1 and r_2 are a mixture of first shell H atoms directed away from the anion and second shell H atoms. Due to the rapid ($1/r^2$) distance falloff, the electric field from the anion has little effect beyond r_2, for which the calculated electric field distribution is essentially identical to that of pure water.

in $g_{HX}(r)$, respectively (see Figure 2). The former group ($r < r_1$) mainly comprises H atoms proximal to the anion and directed to form nearly linear OH···X hydrogen bonds. The arrangement of corresponding water molecules about the ion varies considerably across the halide series. Fluoride has a very well-defined first solvation shell in which the average OH···X angle and distance vary by only about 5° and 0.24 Å, respectively. At the opposite extreme, I^- has a less structured solvation shell wherein the average OH···X angle and distance vary by about 15° and 0.5 Å, respectively.

The second set of H atoms ($r_1 < r < r_2$), situated on average about 1.5 Å farther from the ion, includes water molecules in both the ion's first and second solvation shells. H atoms in this distance range that belong to first shell molecules are generally oriented away from the ion, while those belonging to second shell molecules are generally directed toward the ion. Such distinctions can be drawn clearly in the case of F^-. Overlap of solvation shells surrounding I^-, on the other hand, permits only loose classifications of this sort. Figure 3 summarizes the spatial arrangement of H atoms about a typical halide anion and illustrates the significance of the divisions described above.

Electric field distributions calculated for these two sets of H atoms, $P(E)_{r<r_1}$ and $P(E)_{r_1<r<r_2}$, are plotted in Figures 4 and 5. Histograms of E for H atoms further removed from the ion are nearly indistinguishable from those of pure solvent. Because E is closely related to instantaneous vibrational frequency, this

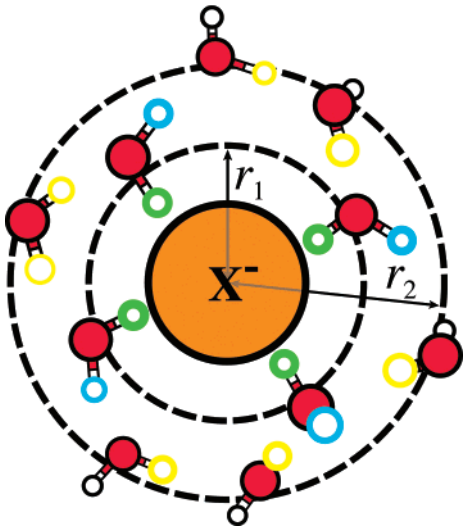

Figure 3. Schematic depiction of an anion's molecular environment. The circular dashed lines at distances r_1 and r_2 represent the first and second minima in the H−X radial distribution function (see Figure 2). The different types of H atoms have been color coded for reference. The green H atoms determine the distribution $P(E)_{r<r_1}$, while blue and yellow H atoms together determine the distribution $P(E)_{r_1<r<r_2}$.

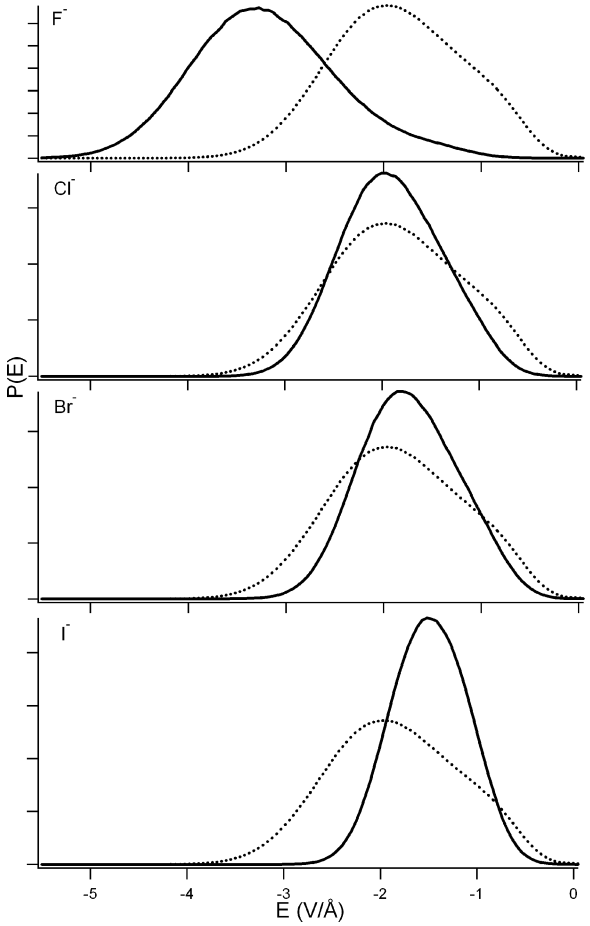

Figure 4. Calculated electric field distributions $P(E)_{r<r_1}$ for H atoms in the first solvation shell at H−X distances less than r_1 (solid lines) compared with the electric field distribution for pure water (dotted line). These H atoms form nearly linear OH···X bonds and are colored green in Figure 2. The large shift in electric field calculated for F^- is consistent with the smaller H−F^- distance compared with those of other anions (see Figure 1).

fact suggests that the Raman spectrum reflects only changes in force and structure very near the ions.

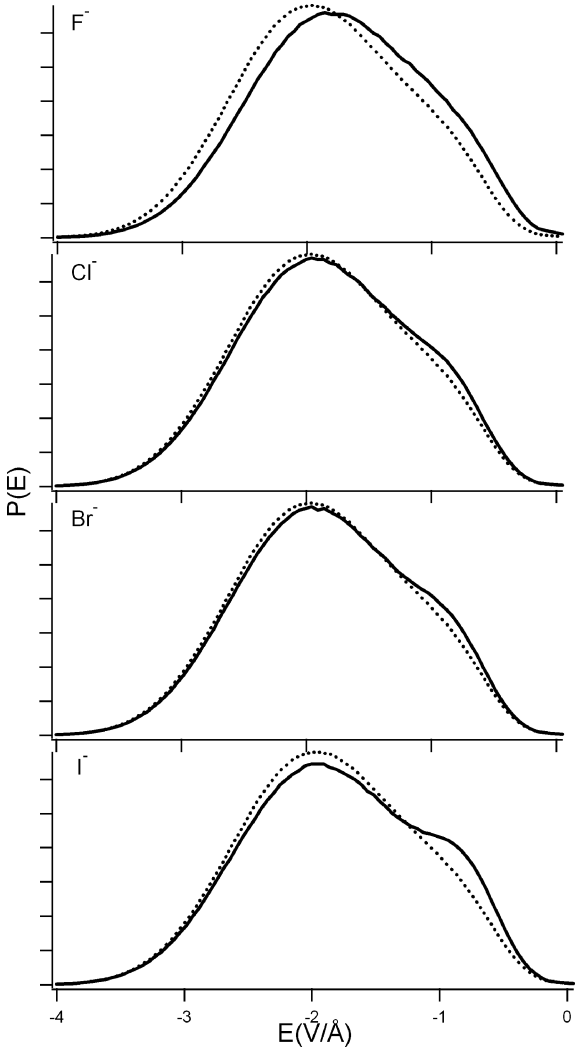

Figure 5. Calculated electric field distributions $P(E)_{r_1<r<r_2}$ for H atoms in the first and second solvation shell located at H−X distances between r_1 and r_2 (solid lines) compared with the electric field distribution for pure water (dotted line).

In the absence of salt, the electric field component E experienced by a typical H atom receives by far the largest contribution from its hydrogen-bonding partner.[12,13] This dominance arises both from the HB acceptor's proximity and from strong alignment of the covalent OH bond along the field exerted by the accepting O atom. Since H atoms adjacent to an anion ($r < r_1$) experience a very different electrostatic environment, one expects their electric field distribution $P(E)_{r<r_1}$ to differ considerably from that of pure solvent. Results shown in Figure 4 confirm this expectation. The average magnitude of E decreases across the halide series with increasing ionic radius. At one extreme, the close approach of H atoms permitted by F^- yields electric fields larger in magnitude than typical fields exerted by a HB-accepting water molecule, and $P(E)_{r<r_1}$ is accordingly shifted to more negative values of E. At the opposite extreme, I^- and Br^- exclude solvent from regions where the ionic field exceeds that of a molecular HB acceptor, and $P(E)_{r<r_1}$ is shifted to less negative values. This fact does not imply that the solvation energy of I^- is less favorable than that of a water molecule, since electrostatic potential energy decays less rapidly with distance than does the field strength itself. Furthermore,

the average coordination number of I^- is roughly twice that of a water molecule.

More surprising is the fact that the breadth of $P(E)_{r<r_1}$ decreases with increasing radius, and therefore with increasing variability in solvation structure. In fact, this anticorrelation reflects little more than the inverse square dependence of an ion's electric field on distance. Because this decay is nonlinear, a given range of H···X separation spans different ranges of field strength at different distances. The enhanced dispersion in $1/r^2$ at short distances is more than sufficient to offset modest broadening of the first hydration shell across the halide series from F^- and I^-. Trends in the mean and variance of $P(E)_{r<r_1}$ thus both follow directly from changes in average H···X distance, which is, in turn, a simple linear function of ionic radius.[25]

H atoms corresponding to the second peak in $g_{HX}(r)$ exhibit more subtle salt-induced changes in computed electric field statistics (see Figure 5). For all halides, the most likely value of E is smaller in magnitude than in pure solvent, with the largest shift produced by F^-. Additionally, the shoulder on the low-field side of the distribution (near -0.8 V/Å) is more pronounced than in pure solvent, with the largest enhancement produced by I^-. These small changes can be readily understood in terms of structure and flexibility of the first two hydration shells, as we explain below.

The ionic field effects a small positive shift in E for protons in the distance range $r_1 < r < r_2$ that belong to molecules in the first solvation shell (shown in blue in Figure 3, and pointing slightly away from the ion, average X···OH angle ~110°). The shift is largest for F^-, both because H···X distance is small and because crowding inhibits formation of HBs between molecules in the first solvation shell (which would reduce the projection of the ionic field onto the OH bond vector). As ionic radius increases across the halide series, H···X distances increase, and molecular crowding abates, systematically attenuating the positive shift in E. The ion shifts E in the opposite direction for H atoms in this distance range that belong to water molecules in the second solvation shell (colored yellow in Figure 5). These protons are responsible for the enhanced shoulder in $P(E)$ near -0.8 V/Å, the origin of which will be discussed in detail below.

Rather than simulate 1 M salt solutions, we constructed Raman spectra to compare with experiment by reweighting electric field distributions of a dilute solution. Assuming that each water molecule in a 1 M solution feels the effects of at most one anion, the Raman scattering intensity corresponding to a given value of E is

$$P(E)_{1M} = \alpha \cdot X_{r<r_1} \cdot P(E)_{r<r_{11}} + X_{r_1<r<r_2} \cdot P(E)_{r_1<r<r_2} + X_{r>r_2} \cdot P(E)_{r>r_2} \quad (3)$$

The statistics of protons in various ranges of distance from the ion contribute to $P(E)_{1M}$ in proportion to their relative populations, i.e., $X_{r<r_1}$, $X_{r_1<r<r_2}$, $X_{r>r_2}$ are the mole fractions of H atoms in the regions $r < r_1$, $r_1 < r < r_2$, and $r > r_2$, respectively. The fraction of H atoms (X) in each distribution was calculated directly from our simulations and the known density of each 1 M salt solution.[25] Finally, the contribution of protons adjacent to the ion, $r < r_1$, is further weighted by the relative Raman intensity (α). We assume that Raman intensities of all other H atoms are unaffected by the anion. Table 1 lists all of the parameters used in eq 3 for each anion.

Table 1. Parameters Used in Eq 3 for Computing the Total Electric Field Distribution for an "Effective" 1 M Solution of Each Halide Ion[a]

X	α	$X_{r<r_1}$	$X_{r_1<r<r_2}$	$X_{r>r_2}$	N_{HB}
I^-	2.956	0.074	0.138	0.789	3.24
Br^-	2.406	0.067	0.132	0.800	2.96
Cl^-	1.884	0.065	0.117	0.817	2.93
F^-	0.71	0.059	0.082	0.858	2.92

[a] Here, α is the relative Raman intensity, and X is the average fraction of H atoms residing in each distance range. The average coordination number (N_{HB}) for water molecules in the first solvation shell of each anion are also included. N_{HB} was determined using a radial cutoff of 3.2 Å.

Raman scattering intensities estimated according to eq 3 are shown in Figure 6 as a function of electric field. Without specifying the proportionality between E and $\Delta\omega$, we can only compare band *shapes* and ion-induced shifts with experimental results. Furthermore, the intensity of the experimental spectra shown in Figure 6A are scaled (using α and X) in a manner identical to that of the calculated electric field distributions. Therefore, as noted, only the band shapes and relative positions, not relative intensities, should be compared. In accord with experimental spectra, the scattering intensity for I^-, Br^-, and Cl^- peaks at weaker (less negative) field and spans a narrower range of field strengths, as compared with pure solvent. The changes induced by F^-, including a slight increase in line width, are much less pronounced, due to the diminished transition polarizability of OH oscillators adjacent to the small ion (see Table 1).

In order to more directly focus on the perturbing effect of the addition of salt on the Raman spectrum of water, we have also calculated difference spectra for each salt (Figure 6A). Specifically, we subtracted the pure HOD/D_2O Raman spectra from the 1 M KX spectra (the spectra are scaled as shown in Figure 6A). The resulting difference spectra represent contributions from only those HOD molecules strongly affected by the addition of salt. The shape and relative position of these spectra can be compared with the reweighted difference electric field distributions ($P(E)_{Diff}$) (Figure 6B), which include only the first two terms in eq 3:

$$P(E)_{Diff} = \alpha \cdot X_{r<r_1} \cdot P(E)_{r<r_{11}} + X_{r_1<r<r_2} \cdot P(E)_{r_1<r<r_2} \quad (4)$$

As shown in Figure 6, the reweighted difference electric field distributions also reproduce the experimental difference spectra remarkably well. Agreement with experiment is most striking for the larger halides, such as I^-, which shows a clear asymmetry on the strong electric field (lower vibrational frequency) side of the distribution (spectrum). While the basic shape and position of the I^- reweighted difference electric field distribution is determined by the electric field at H atoms directly bonded to the anion, the asymmetric peak shape arises from protons that are near, but not adjacent to, the anion (i.e. $P(E)_{r_1<r<r_2}$), which experience slightly stronger fields than in pure solvent (see Figures 4 and 5). Both the difference spectrum and the reweighted difference electric field distribution for F^- are quite broad. This broadening is due to the fact that $P(E)_{r<r_1}$ and $P(E)_{r_1<r<r_2}$, which determine the reweighted difference distribu-

(25) Lide, D. R., Ed. Properties of Solids. In *CRC Handbood of Chemistry and Physics*, Internet Version; Taylor and Francis: Boca Raton, FL, 2006.

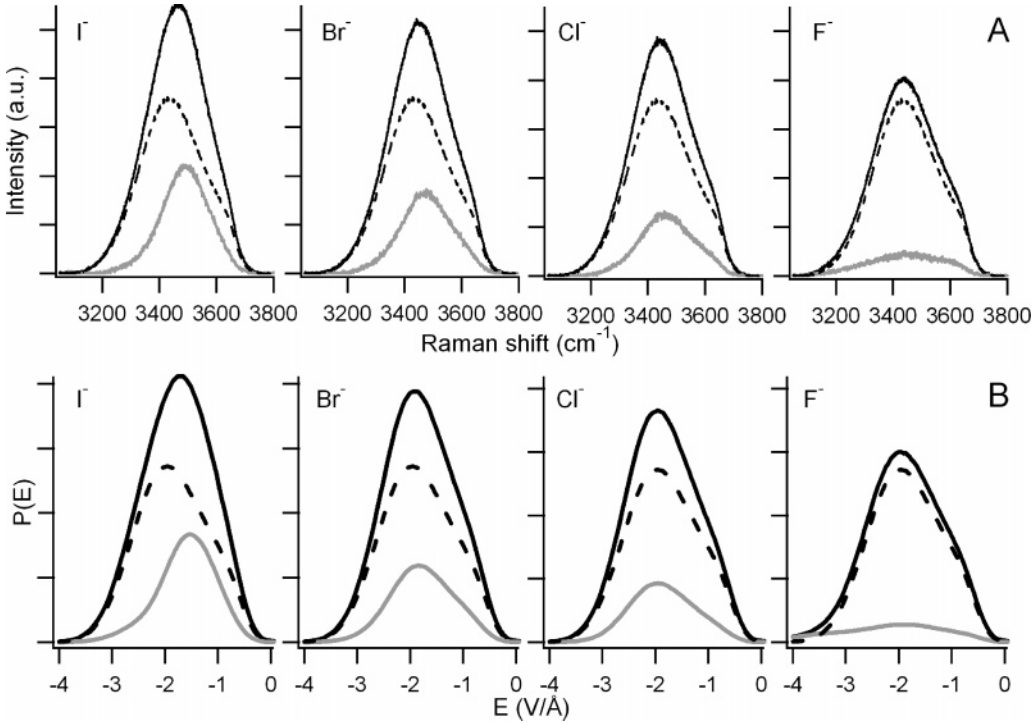

Figure 6. (A) Measured Raman spectra (solid black lines) of 1 M KX, the Raman spectrum of pure HOD/D_2O (dashed line), and the difference spectrum for each salt (solid gray line). (B) Calculated electric field distributions for an "effective" 1 M solution (solid black lines) of each anion, the electric field distribution for pure water (dashed line), and the difference electric field distributions for each anion (solid gray lines). Difference spectra are calculated by subtracting the pure HOD/D_2O spectrum, scaled by $X_{r>r_2}$, from the 1 M KX spectrum, which is scaled by $(\alpha \cdot X_{r<r_1} + X_{r_1<r<r_2} + X_{r>r_2}$.

tion (see eq 4), are shifted in opposite directions. However, the peak width for F^- is somewhat overestimated by our calculations, as compared to experiment. This discrepancy is not necessarily surprising, given that we have only considered purely electrostatic effects, whereas charge transfer to the solvating water molecules is known to be most significant for F^-.[26]

Because the electric field component E is nearly proportional to shifts in vibrational frequency,[12−14] the *shape* of its equilibrium distribution $P(E)$ can be directly compared to experimental Raman spectra. In order to plot $P(E)$ alongside spectral data, we have selected a proportionality coefficient that yields close agreement in the absence of ions. In detail, we converted E to vibrational frequency using eq 1, for which the slope (Q) and intercept (ω_0) were determined by fitting $P(E)$ for pure water to the Raman spectrum of HOD in D_2O (see Figure 7). The resulting best fit equation was found to be

$$\omega = \frac{160.514\ \mathrm{cm}^{-1}}{\mathrm{V/Å}} \cdot E + 3745\ \mathrm{cm}^{-1} \qquad (5)$$

Equation 5 was then used to convert the reweighted electric field distributions for each ion ($P(E)_{1M}$ and $P(E)_{Diff}$) to vibrational frequency distributions (Figure 8), always using the same slope and intercept determined for pure water. The primary purpose of Figure 8 is to further show that the shapes and relative positions of our measured Raman spectra are well represented by the reweighted electric field distributions. Given the complete neglect of dynamical effects, the correspondence between theory and experiment is remarkable.

The congruence of measured Raman spectra and calculated $P(E)$ band shapes (Figure 8) calls into question conventional

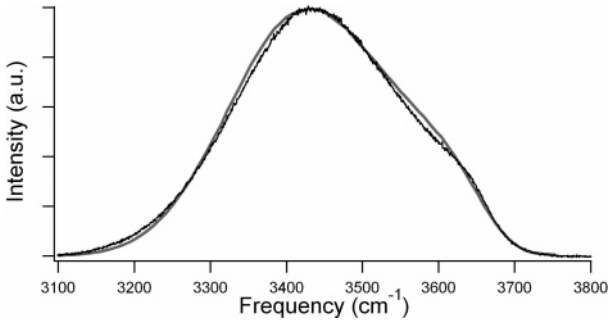

Figure 7. Direct comparison of the experimental Raman spectrum for pure HOD in D_2O with the calculated electric field distribution, which has been converted to a vibrational frequency distribution using eq 5. The parameters of eq 5 (slope and intercept) were chosen in order to give good agreement with the experimental Raman spectrum.

interpretations of the influence that anions have on OH vibrational spectra. Changes in *P(E) do not reflect the large HB network rearrangements* implied by designations of "structure making" and "structure breaking" ions. Instead, they manifest the electric field an ion exerts on nearby hydrogen atoms. Since the anion exerts large electrostatic forces only on water molecules in the first solvation shell, and to a much smaller extent the second solvation shell, Raman spectra are, in fact, rather insensitive to collective structural rearrangements. On the basis of Raman measurements alone, we can thus infer little about molecular organization beyond the immediate vicinity of an ion.

This insensitivity of Raman spectroscopy to structural rearrangements does not, of course, limit our computer simulation studies, which provide a detailed view of solvation structure at all microscopic distances. An inability to draw quantitative comparisons with experiment simply limits the confidence with

(26) Robertson, W. H.; Johnson, M. A. *Annu. Rev. Phys. Chem.* **2003**, *54*, 173.

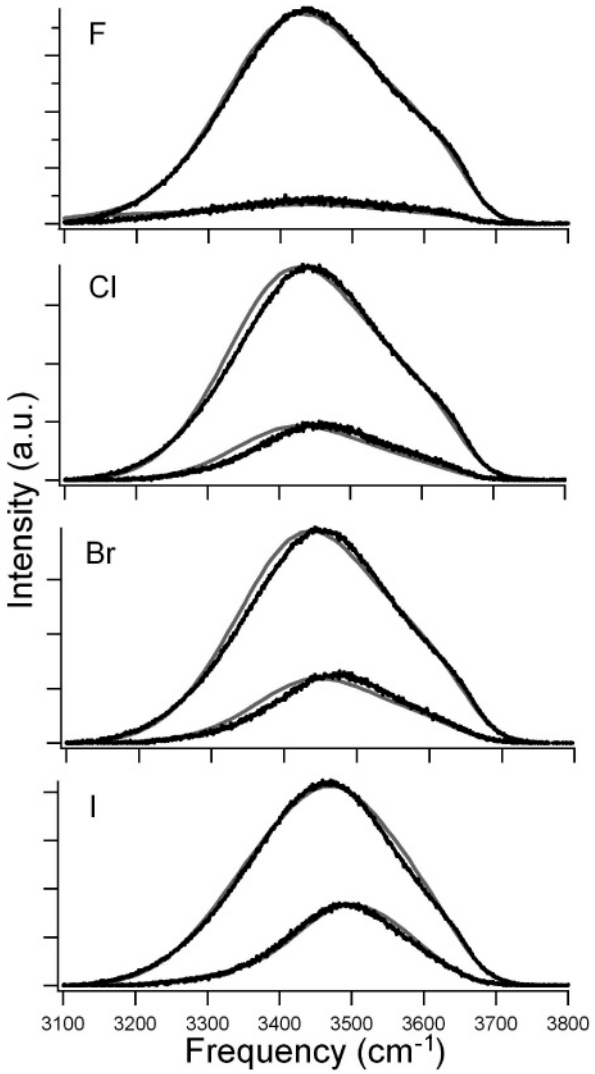

Figure 8. Measured Raman spectra and the difference spectrum for each salt (solid black lines), directly compared with electric field distributions for an "effective" 1 M solution and the difference electric field distributions for each anion (solid gray lines). Electric field has been converted to vibrational frequency using eq 5.

which we can draw conclusions based upon empirical models of molecular interactions. We investigated ion-induced structural changes from simulations by collecting statistics of the simplest local geometric parameter for HB strength, namely the distance r_{OH} between a hydrogen atom and the nearest (but not covalently bound) oxygen atom within a cone of width $\pi/3$.[15] Figure 9 shows distributions of this parameter for H atoms near I^- and F^-, as well as that for H atoms distant from an ion (which is indistinguishable from the distribution calculated for pure water). We focus here exclusively on F^- and I^- because they are representative of the range of observed effects, whereas Cl^- and Br^- constitute intermediate cases. It is clear from Figure 9 that local configurations of HBs involving H atoms near, but not adjacent to, the anion are in fact very similar to HB interactions in pure water. Nonetheless, a small degree of HB distortion is noticeable for both F^- and I^-, as evidenced by the small shift in weight from shorter/stronger HBs ($r_{OH} \approx 1.8$ Å) to longer/weaker HBs ($r_{OH} > 2.2$ Å). The shift is slightly more pronounced for I^- than for F^-, as reflected by the high-field shoulders of the corresponding electric field distributions, $P(E)_{r_1<r<r_2}$ (Figure 5). This distinction can be rationalized in

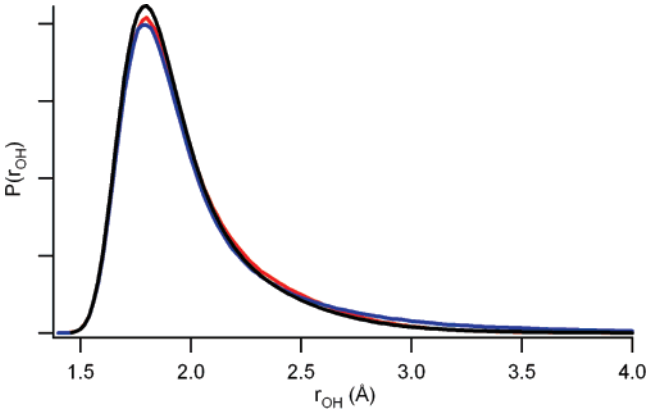

Figure 9. Calculated r_{OH} distributions for H atoms located at H−X distances between r_1 and r_2 ($P(r_{OH})_{r_1<r<r_2}$) for I^- (blue line) and F^- (red line) compared with the r_{OH} distribution for pure water (black line). The r_{OH} distributions for Br^- and Cl^- are intermediate between I^- and F^-. It is clear that only a very small degree of HB distortion results from the anions' presence.

terms of crowding in the ions' immediate environments. Average coordination numbers for water molecules in each ion's first solvation shell, listed in Table 1, indicate a high degree of compaction in the vicinity of F^-, relative to the other halide anions. Perhaps more strikingly, the accessible surface area of I^-, based on ionic radii, is nearly three times that of F^-. Despite its greater size, the first coordination shell of I^- accommodates, on average, just one more water molecule than that of F^-. Ample space is therefore readily available for more distant (second shell) water molecules to directly interact with I^-, unobstructed by intervening molecules. As a result, second shell H atoms nearest the anion (yellow H atoms in Figure 3) are strongly oriented toward I^-, at the expense of forming strong HBs with other water molecules. By contrast, the tight coordination structure of F^- effectively screens second shell water molecules from the anion, preventing any substantial direct interactions. In the case of F^-, deviations of $P(r_{OH})_{r_1<r<r_2}$ away from the pure solvent are instead associated with first shell H atoms directed away from the anion (green H atoms in Figure 3). Close approach of the small anion's first coordination shell orients those molecules so rigidly that they cannot fully adapt to the surrounding HB environment. However, we stress that the distortions in both instances are small ones.

In summary, we observe only small HB distortions (relative to pure water) for H atoms near both I^- and F^-, but the origin of this distortion is different for I^- (second shell H atoms) compared with that for F^- (first shell H atoms). However, we find that this small distortion, which is evidenced in the electric field distribution by a small increase in the shoulder intensity, is only weakly reflected in the Raman spectrum. *The most pronounced changes in the Raman spectrum due to dissolved salt primarily result from the electric field effects on first shell H atoms directly bonded to the ion.* This is demonstrated in Figure 10, which shows the electric field distribution for an "effective" 1 M solution, in which the electric field from the first shell H atoms directly bonded to the anion ($P(E)_{r<r_1}$) is not included. It is clear that the shape of such an "effective" 1 M electric field distribution is nearly identical to that of pure water, thus indicating that the effect on the spectrum from OH oscillators not directly bonded to the anion is indeed minimal. These results contradict the classification of halide anions as either "structure makers" or "structure breakers". In fact, we

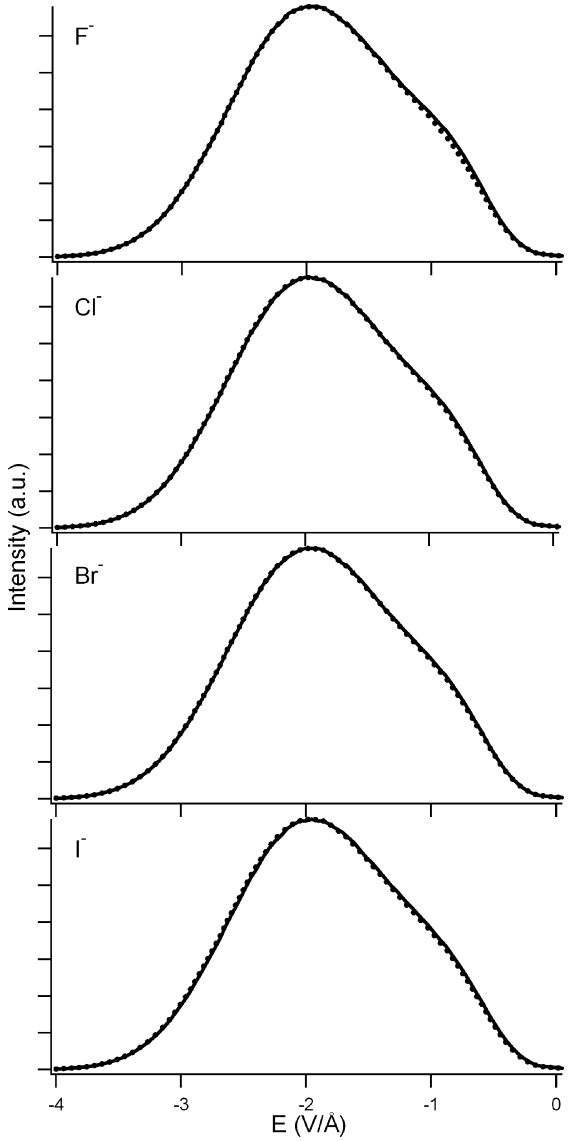

Figure 10. Comparison of the "effective" 1 M electric field distribution (solid black line) with the electric field distribution for pure water (dashed gray line). Here the "effective" 1 M distribution does not include contributions from the first shell H atoms directly bonded to the anion ($P(E)_{r<r_1}$). For each anion studied this "effective" 1 M electric field distribution is very similar to the electric field distribution for pure water. This similarity indicates that the observed changes in the Raman spectrum are primarily the result of first shell H atoms directly associated with the anion.

find that the differences in the observed 1 M KX Raman spectra predominately reflect the different anionic radii, as opposed to distinct structural perturbations.

Local HB configurations are only one aspect of intermolecular structure in liquid water. The weak effect of halide anions on HB strengths in our simulations belies a pronounced influence on more collective features of molecular organization. To highlight such concerted rearrangements, we discriminate between direct and indirect consequences of the ion's presence on outer solvation shell structure. Each ion recruits a shell of coordinating water molecules whose arrangement is highly atypical of pure solvent. These densely packed and strongly oriented molecules act as a kind of boundary for the remaining solvent. The effect of this inner shell boundary on outer solvation shells, independent of the ion's long-ranged electric field, we

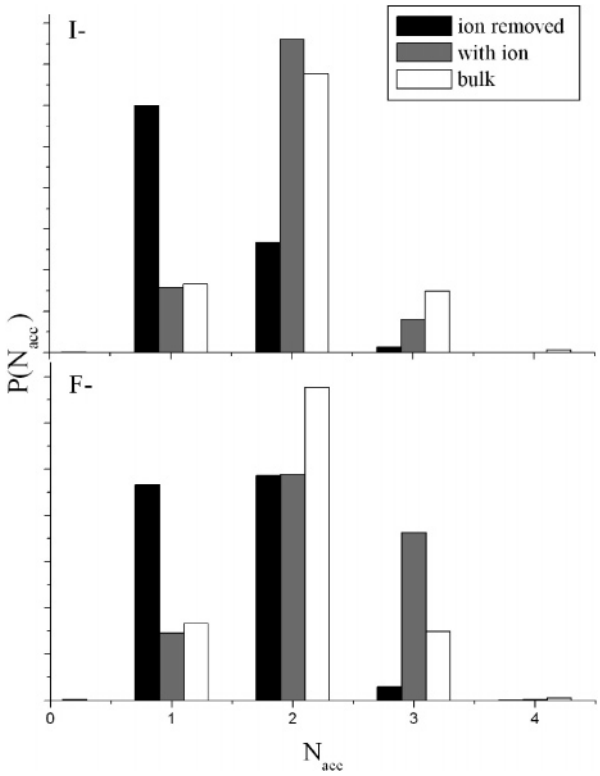

Figure 11. Histograms of the number of HBs accepted by first shell water molecules. The data labeled "ion removed" correspond to simulations in which a handful of molecules is constrained to the geometry of an ion's first solvation shell, but in which the ion itself is absent. Oxygen atoms in the first solvation shell accept markedly fewer HBs in this case than in pure water. When the ion is restored, so that all water molecules experience its electric field, these O atoms exhibit HB statistics very similar to pure solvent.

designate as indirect. Direct effects arise instead from electrostatic forces exerted by the ion on outer shell molecules, independent of inner shell structure. In order to scrutinize direct and indirect influences of the anion separately, we have performed simulations in which the ion is absent, but the first solvation shell is structured as if the ion were present. In detail, we sample configurations of the inner shell from the aqueous halide simulations already described. Each of these configurations is used as a rigid "solute" in subsequent simulations of liquid water, in which no ion is present. Differences between liquid structure around this fixed shell of molecules and that of pure liquid water indicate indirect effects of ion solvation. Differences between liquid structure around the fixed shell of molecules and that around a fully represented ion point to direct effects of ion solvation.

HB statistics obtained from our ion-free simulations with imposed coordination shell, shown in Figure 11, reveal that the indirect influence of halide ions is strong and generally opposes their direct influence. Because they are highly oriented, inner shell water molecules can donate only one hydrogen bond to their surroundings, while they may accept two or possibly more. This local imbalance provides H atoms in the range $r_1 < r < r_2$ diverse opportunities to form strong HBs, as shown by the histograms of the number of HBs accepted by first shell O atoms (N_{acc}) plotted in Figure 11. Distributions of r_{OH}, plotted in Figure 12, indicate that second shell H atoms indeed engage in strong HBs more frequently than H atoms in the pure liquid. In contrast, direct structural effects of the ion's electric field include

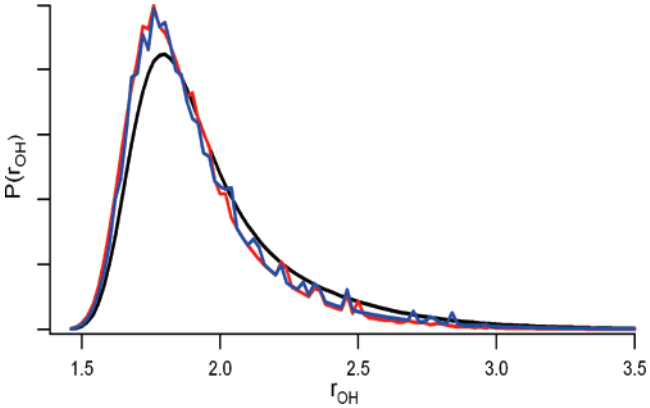

Figure 12. Calculated distributions of HB distance r_{OH} in simulations with "ion cavities", compared with the r_{OH} distribution for pure water (black line). The blue line corresponds to a solute surrounded by the first solvation shell of an I^- that does not exert forces on more distant solvent molecules. The red line corresponds to a similar solute with the first solvation shell of F^-. Distributions for these two solutes include only contributions from H atoms in the distance range $r_1 < r < r_2$. In both cases HB structure is slightly enhanced near the imposed solvation shell.

contraction of outer solvation shells, and bias of their OH orientations toward the ion. Both effects increase the number of H atoms in the range $r_1 < r < r_2$, reversing the local imbalance of donors and acceptors. The greater competition for available HB acceptors results in slightly weaker, more distorted HBs on average than in the pure liquid.

Structure induced by an anion's coordination shell and the ion's long-range electric field both substantially perturb the spatial pattern of molecules in outer shells. It is remarkable that neither perturbation (nor their combination) significantly reduces the number or typical strength of HBs. Such resilience of water's HB network has been described in other contexts as well, for example, the hydrophobic effect.[27] Even an ideal hydrophobic sphere must span nearly a nanometer in order to break HBs with high probability. Although liquid water is characterized by locally tetrahedral geometry, fluctuations about ideal HB configurations (including angular distortions as well as over-coordination of HB acceptors) provide sufficient flexibility to accommodate substantial variations in density and HB donor/acceptor abundance. It is, of course, possible to perturb the HB network beyond this linear response regime, as do very large hydrophobic solutes[27] and perhaps highly charged ions, but in our model, the halide anions F^-, Cl^-, Br^-, and I^- do not.

(27) Chandler, D. *Nature* **2005**, *437*, 640.

Conclusions

Through a detailed comparison of experimental Raman spectral measurements with classical MC simulations, we have shown that the strong perturbations to the vibrational spectrum of water effected by the addition of potassium halides is a direct result of the electric fields that anions exert on adjacent H atoms. This result contrasts with the widely held interpretation that such spectral changes signify structural rearrangements in the HB network. In fact, analysis of our simulations reveals that halides induce only minor HB distortions beyond the adjacent shell of coordinating OH groups. The physical origin of these small distortions varies within the halide series but generally illustrates the ability of water's HB network to withstand the very large forces imposed by small ions and their immediate coordination shells.

Acknowledgment. This work was supported by the Chemical Sciences, Geosciences, and Biosciences Division of the U.S. Department of Energy. Gaussian calculations and MC simulations were performed at the UC Berkeley College of Chemistry Molecular Graphics and Computation Facility (NSF Grant No. CHE-0233882).

Supporting Information Available: Complete ref 21. This material is available free of charge via the Internet at http://pubs.acs.org.

JA071933Z